

USAFSAM-TR-85-86

11

RADIATION DOSES FROM FLYING THROUGH NUCLEAR DEBRIS CLOUDS

AD-A167 959

Peter M. Vanden Bosch, Second Lieutenant, USAF

Arthur Woodrum, Ph.D.

April 1986

Final Report for Period 2 January - 10 January 1985

DTIC
SELECTED
MAY 30 1986
S D
A f

Approved for public release; distribution is unlimited.

DTIC FILE COPY

USAF SCHOOL OF AEROSPACE MEDICINE
Aerospace Medical Division (AFSC)
Brooks Air Force Base, TX 78235-5301



REPORT DOCUMENTATION PAGE

1a. REPORT SECURITY CLASSIFICATION UNCLASSIFIED			1b. RESTRICTIVE MARKINGS		
2a. SECURITY CLASSIFICATION AUTHORITY			3. DISTRIBUTION/AVAILABILITY OF REPORT Approved for public release; distribution is unlimited.		
2b. DECLASSIFICATION/DOWNGRADING SCHEDULE					
4. PERFORMING ORGANIZATION REPORT NUMBER(S) USAFSAM-TR-85-86			5. MONITORING ORGANIZATION REPORT NUMBER(S)		
6a. NAME OF PERFORMING ORGANIZATION USAF School of Aerospace Medicine		6b. OFFICE SYMBOL (if applicable) USAFSAM/RZB	7a. NAME OF MONITORING ORGANIZATION		
6c. ADDRESS (City, State, and ZIP Code) Aerospace Medical Division (AFSC) Brooks Air Force Base, TX 78235-5301			7b. ADDRESS (City, State, and ZIP Code)		
8a. NAME OF FUNDING/SPONSORING ORGANIZATION USAF School of Aerospace Medicine		8b. OFFICE SYMBOL (if applicable) USAFSAM/RZB	9. PROCUREMENT INSTRUMENT IDENTIFICATION NUMBER		
8c. ADDRESS (City, State, and ZIP Code) Aerospace Medical Division (AFSC) Brooks Air Force Base, TX 78235-5301			10. SOURCE OF FUNDING NUMBERS		
	PROGRAM ELEMENT NO. 62202F	PROJECT NO. 7757	TASK NO. 04	WORK UNIT ACCESSION NO. 42	
11. TITLE (Include Security Classification) RADIATION DOSES FROM FLYING THROUGH NUCLEAR DEBRIS CLOUDS					
12. PERSONAL AUTHOR(S) Vanden Bosch, Peter M.; Woodrum, Arthur (Professor, Georgia Southern University).					
13a. TYPE OF REPORT Final		13b. TIME COVERED FROM 1/2/85 TO 1/10/85		14. DATE OF REPORT (Year, Month, Day) 1986, April	15. PAGE COUNT 21
16. SUPPLEMENTARY NOTATION					
17. COSATI CODES			18. SUBJECT TERMS (Continue on reverse if necessary and identify by block number)		
FIELD	GROUP	SUB-GROUP	Post-blast nuclear radiation; Radiation dosage; Nuclear weapon debris; Fallout prediction; Cloud penetration		
15	06				
19. ABSTRACT (Continue on reverse if necessary and identify by block number) Taboada et al. have recently developed a computer model to predict gamma-radiation doses to aircrews flying through nuclear debris clouds. Although the model has the advantages of taking a large number of parameters into account and using the benchmark DELFIC code to model cloud dynamics, it takes up to 20 min for a single run on a mainframe computer. Results from a number of runs have been generalized into empirical formulae. From these results it is possible to estimate worst case gamma-radiation doses for complex scenarios using a hand calculator.					
20. DISTRIBUTION/AVAILABILITY OF ABSTRACT <input checked="" type="checkbox"/> UNCLASSIFIED/UNLIMITED <input type="checkbox"/> SAME AS RPT <input type="checkbox"/> DTIC USERS			21. ABSTRACT SECURITY CLASSIFICATION UNCLASSIFIED		
22a. NAME OF RESPONSIBLE INDIVIDUAL Peter M. Vanden Bosch, 2Lt, USAF			22b. TELEPHONE (Include Area Code) (512) 536-3416	22c. OFFICE SYMBOL USAFSAM/RZB	

TABLE OF CONTENTS

	<u>Page</u>
INTRODUCTION.	1
FLYTHROUGH MODEL.	1
CLOUD DIMENSIONS.	2
DUST CLOUD CHARACTERISTICS.	4
DOSE AT THE END OF FLYTHROUGH	4
POST FLYTHROUGH DOSE.	6
CONCLUSIONS	9
ACKNOWLEDGMENTS	11
REFERENCES.	11
APPENDIX A: CORRECTION FOR AIRCRAFT PARAMETERS	13
APPENDIX B: EVALUATION OF MODEL ASSUMPTIONS.	15

Figures

<u>Fig.</u> <u>No.</u>		
1.	Base and Top Heights of Cloud vs. Yield	3
2.	Radius of Cloud vs. Yield	3
3.	Dose vs. Height for a 1 MT Yield.	5
4.	Dose vs. Yield.	5
5.	Dose vs. Time for a 10 MT Yield	6
6.	Dose vs. Time Near Cloud Top.	7
7.	Dose vs. Time Near Cloud Base	7
8.	Rate Constant vs. Time Near Cloud Top	8
9.	Rate Constant vs. Time Near Cloud Base.	9

RADIATION DOSES FROM FLYING THROUGH NUCLEAR DEBRIS CLOUDS

INTRODUCTION

Estimates of radiation doses to aircrews flying through nuclear debris clouds are of critical interest to USAF mission planners. The probability of such an event occurring is high following a nuclear attack. Since real data are lacking, prediction must depend upon mathematical modeling of the cloud environment and flythrough.

Taboada et al. (1) recently developed a computer model which predicts doses from flythroughs. The model, which will be called CASSIE in this report, is based upon the dust environment model CASSANDRA (2), which in turn uses the benchmark DELFIC (3) code as the basis of its cloud rise and fallout dynamics. The CASSIE model is user friendly; it supplies default values and descriptions of parameters when requested and has all the input flexibilities of the DELFIC and CASSANDRA codes.

The CASSIE model uses the CASSANDRA code to calculate the dust density at various points along the trajectory of an aircraft flying through a nuclear debris cloud. A gamma-radiation dose rate is calculated from the dust densities and integrated over time to obtain the total radiation dose that an aircrew would experience.

The total radiation dose is assumed to originate from 2 sources: (1) the immersion radiation dose, which is a result of the aircraft being immersed in a radioactive cloud, and (2) the onboard radiation dose, which results from radiation exposure of the aircrews to dust particles trapped inside the aircraft cabin and filtering system. The immersion rate exists only while the aircraft is inside the radioactive debris cloud, whereas the onboard radiation is a continuing hazard.

The purpose of this report is to use the CASSIE model to calculate the radiation doses to aircrewmembers for various conditions of flythrough. Due to the long program running time, the model would have little use in an operational setting. The intent of this report is to supply results of the model in a form which will allow planners to estimate in advance realistic and worst case doses for flythrough scenarios.

FLYTHROUGH MODEL

CASSIE provides for changing flight and aircraft parameters easily. A scenario is needed which will allow an analysis of radiation dose dependence on height of flythrough, time of flight, and detonation yield. For the purposes of this report, the following flight scenario was used.

An aircraft flies from a point 40 km (24 mi) from ground zero on one side of a detonation to 40 km on the opposite side, passing directly over ground zero. The flight duration is 500 s, which corresponds to a velocity of 311 knots. A height H is maintained throughout the flight and the aircraft passes

over ground zero at t seconds after detonation. This path is expressed in the form $(-40 \text{ km}, 0, H, t-250) - (40 \text{ km}, 0, H, t+250)$.

The aircraft parameters are chosen to resemble those of a KC-135 aircraft. The model approximates the cabin as a cylinder, chosen to be 32.05 m (107 ft) in length and 2.74 m (9 ft) in radius. The filtration system is arbitrarily chosen to allow 50% of the dust particles taken onboard to enter the cabin, with the remainder staying on the filter. Once aboard, the dust particles do not exit. The distance from the crewmembers to the filter is arbitrarily chosen to be 250 cm (100 in.). The air-mass flow into the aircraft is 67.5 kg/min (150 lb/min). The dose received by aircrewmembers will be dependent on the choice of these parameters, which are discussed in Appendix A. If cloud penetration is unavoidable, Figure 3 shows that it is most advantageous to fly through as high in the cloud as possible. This will allow the aircraft to be exposed to the lowest possible dose within the cloud. A flythrough beneath the cloud may result in a lower dose, but there is the danger of the aircraft encountering large particles.

CLOUD DIMENSIONS

The size of the nuclear debris cloud depends on a number of factors. The parameters used in the analysis include:

- (1) A surface burst, with 50% of the available energy expended in fission.
- (2) Ground zero at 670 m (2211 ft) above mean sea level.
- (3) No wind.
- (4) Soil type is siliceous.

The debris cloud is modeled throughout its creation, expansion, and cooling. At some point the model considers the turbulence, upward rise, and expansion to be negligible and stabilizes the cloud dimensions at current values. These calculations are reported in Table 1 and the cloud dimensions are shown in Figures 1 and 2. Stabilization is relative; in actuality, the cloud will continue to grow slowly as a result of buoyancy, turbulence, and wind patterns.

TABLE 1. CLOUD DIMENSION DATA AT STABILIZATION

Yield (MT)	Stab. Time(s)	Cloud Base(m)	Cloud Top	Cloud Radius
0.003	312	3700	5200	1100
0.01	423	5300	7400	1800
0.03	661	6700	10500	2900
0.1	611	8400	12400	5400
0.3	720	9500	14900	8500
1.	783	11300	18000	13800
3.	785	13500	22000	20300
10.	787	17700	29000	31000
30.	852	21000	37200	52400

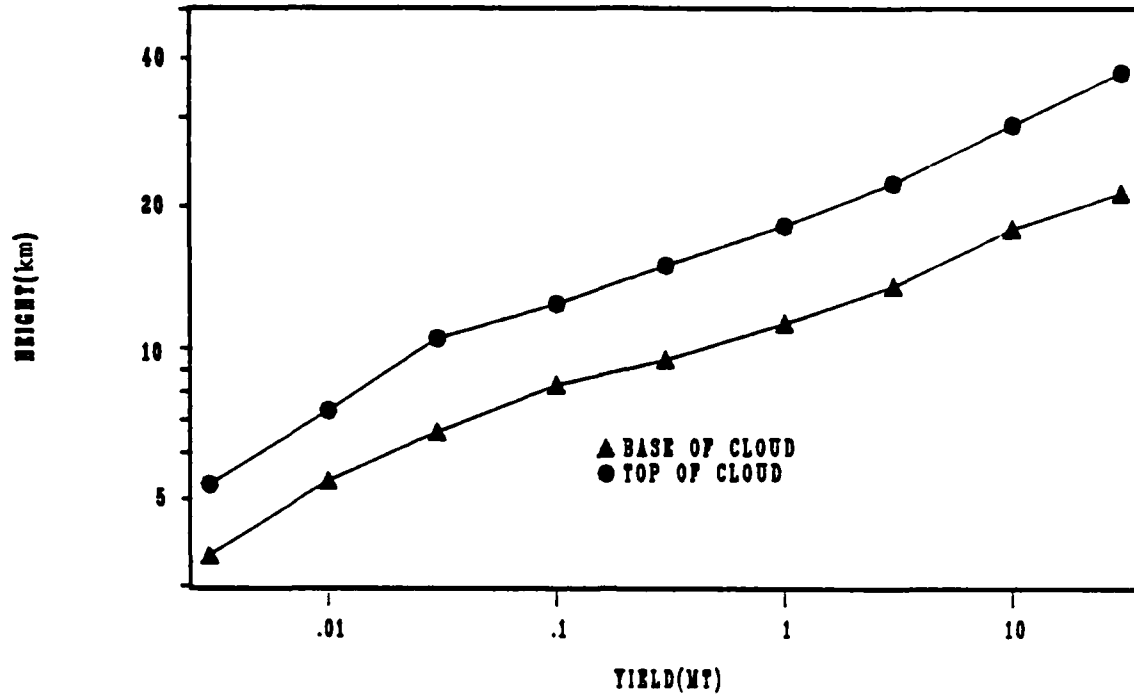


Figure 1. Base and top heights of clouds vs. yield.

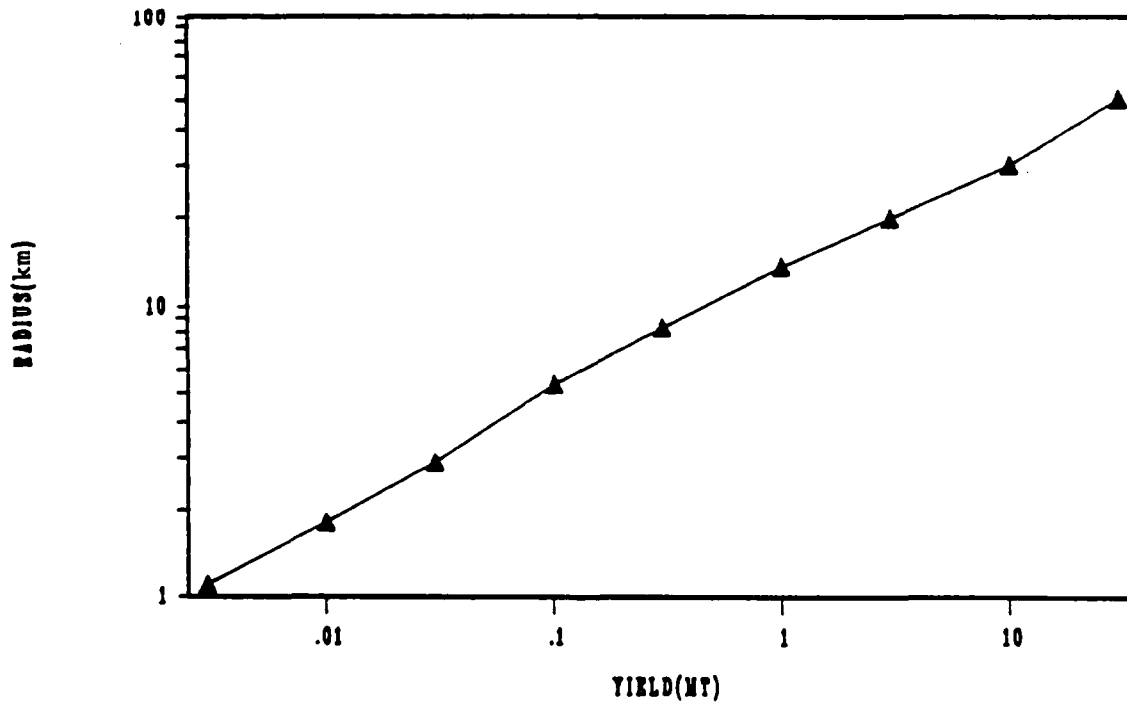


Figure 2. Radius of cloud vs. yield.

These calculations are based on the DELFIC and CASSANDRA portions of the model. The cloud top and bottom heights agree well with values reported by Glasstone and Dolan (4). Cloud radii appear to be larger by as much as a factor of 1.4 than those reported. Part of the disagreement may be explained by the ambiguous nature of the cloud dimensions. Part may be explained by the fact that DELFIC was intended as a ground fallout code, and ground fallout is relatively insensitive to cloud radius or base height choices (7). This is a drawback since flythrough dose is approximately inversely proportional to cloud radius in this model.

DUST CLOUD CHARACTERISTICS

In the model, the mass of soil entrained by the burst is dependent on the height of burst above ground, type of soil, and explosive yield. A log-normal distribution of particle sizes is assumed, and the dust is partitioned into 100 size classes. At initial time the soil burden is distributed uniformly throughout the cloud. As the cloud grows with time, the soil debris will be lofted with the cloud at a rate dependent on particle size. The gamma-radiation rate at each point in the cloud is proportional to the dust mass concentration at that point. The latter assumption is considered in detail in Appendix B.

One way of looking at the vertical distribution of dust is to conduct flythroughs at various heights. Figure 3 shows the dependence of total dose accumulated during the flythrough scenario as height is varied for 3 different times. For T=500 s the flythrough starts 250 s and ends 750 s after burst. The aircraft passes through the entire cloud (radius = 13.8 km (8.4 mi)) before stabilization is reached at 783 s (Table 1). The dose is nearly constant for flythroughs passing through the cloud. As the aircraft flies at heights lower than the cloud base, the dose received is relatively much lower; only large particles have fallen out to those levels. At later times, the dust activity has decayed as well as fallen. The dose received during flights below the cloud base is relatively more substantial.

The flythrough at the cloud base receives the largest dose. In the following analyses, this will be considered as the worst case scenario.

DOSE AT THE END OF FLYTHROUGH

The dose from a flythrough is strongly dependent on the time of flythrough and the yield of the detonation. Figure 4 shows the dose accumulated by the end of the flythrough at the cloud base vs. yield at 1000 s. Although the data on this graph (Fig. 4) do not all lie on a straight line, the data with yields greater than 0.1 MT strongly suggest a power relationship.

Figure 5 shows the dependence of dose at the end of flythrough on time of flythrough. The time plotted is the time after detonation that the aircraft passes over ground zero. Regression lines to these data are also shown. The

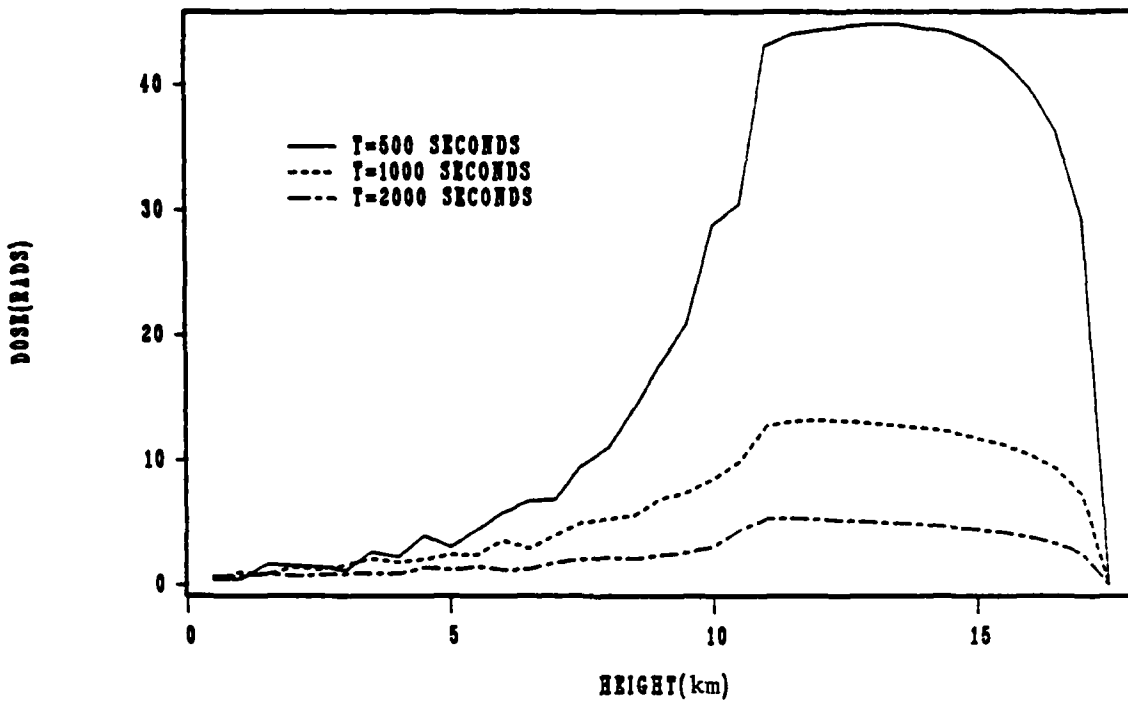


Figure 3. Dose vs. height for a 1 MT yield flythrough.
 (-40 km, 0, H, t-250)-(40 km, 0, H, t+250).

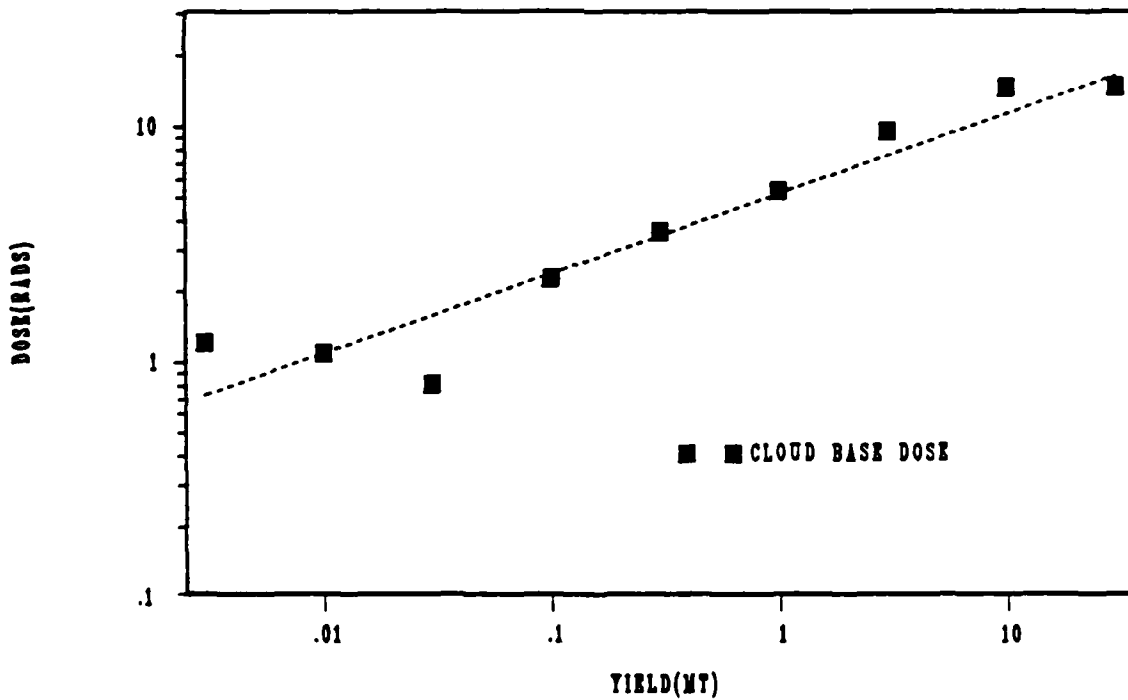


Figure 4. Dose vs. yield.
 Flythrough (-40 km, 0, H, 1750)-(40 km, 0, H, 2250).

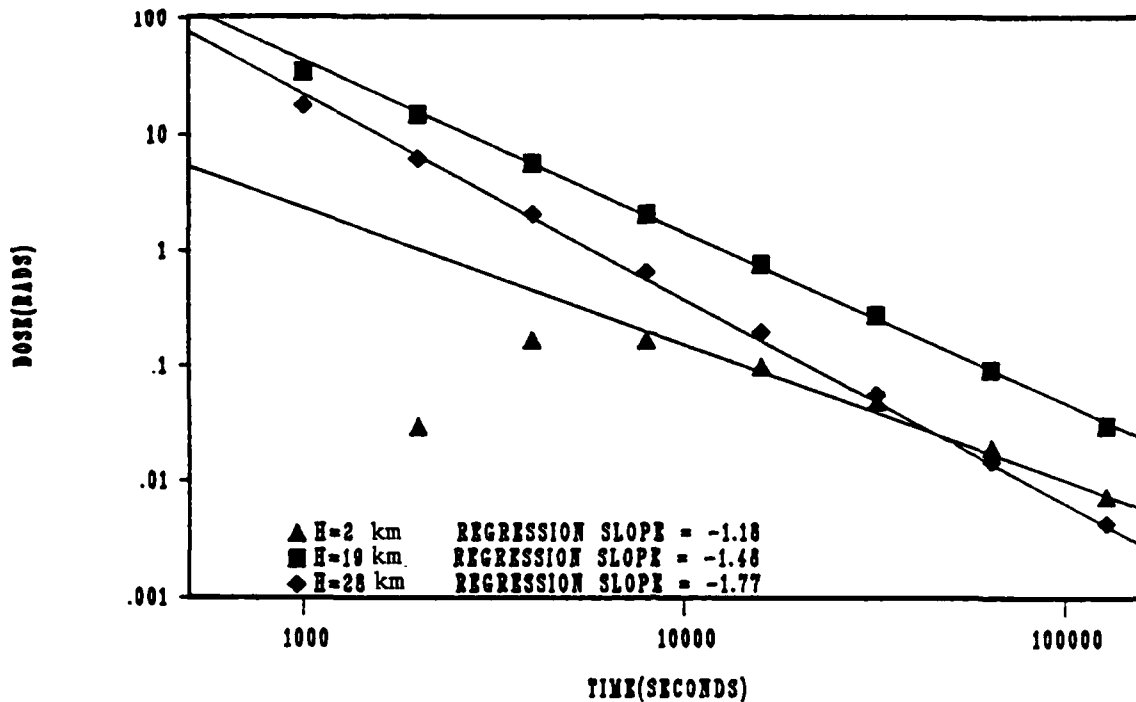


Figure 5. Dose vs. time for a 10 MT yield.
Flythrough (-40km, 0, H, t-250)-(40km, 0, H, t+250)

regression fit to the flythrough at an altitude of 2 km (1.2 mi) does not include the data for the four earliest times. The flythrough at 19-km (11.6 mi) altitude represents a flight through the base of the cloud while the flythrough at 28-km (17.1 mi) altitude is close to the top of the cloud. The power dependence of dose on time is greater than the $t^{-1.2}$ (Way-Wigner (5)) dependence built into the model. This is a result of the dust "falling out" to lower levels.

Figures 6 and 7 show the dependence of dose on time for flythroughs near the cloud top and bottom, respectively. These graphs show that the exponent in the time dependence is nearly independent of yield. A multiple regression on data for times between .5 h and 3 days, for yields above .1 MT, and for flythroughs near the cloud base produces the approximate relationship

$$\text{Dose} = 2.34 W^{.48} t^{-1.53} \quad (1)$$

where W is in megatons and t is in hours. This time dependence compares favorably with the $t^{-1.6}$ dependency observed in actual flythroughs (6).

POST FLYTHROUGH DOSE

The radiation from onboard sources is insignificant (3% of immersion dose) while the aircraft is immersed in the cloud. However, since the onboard dust

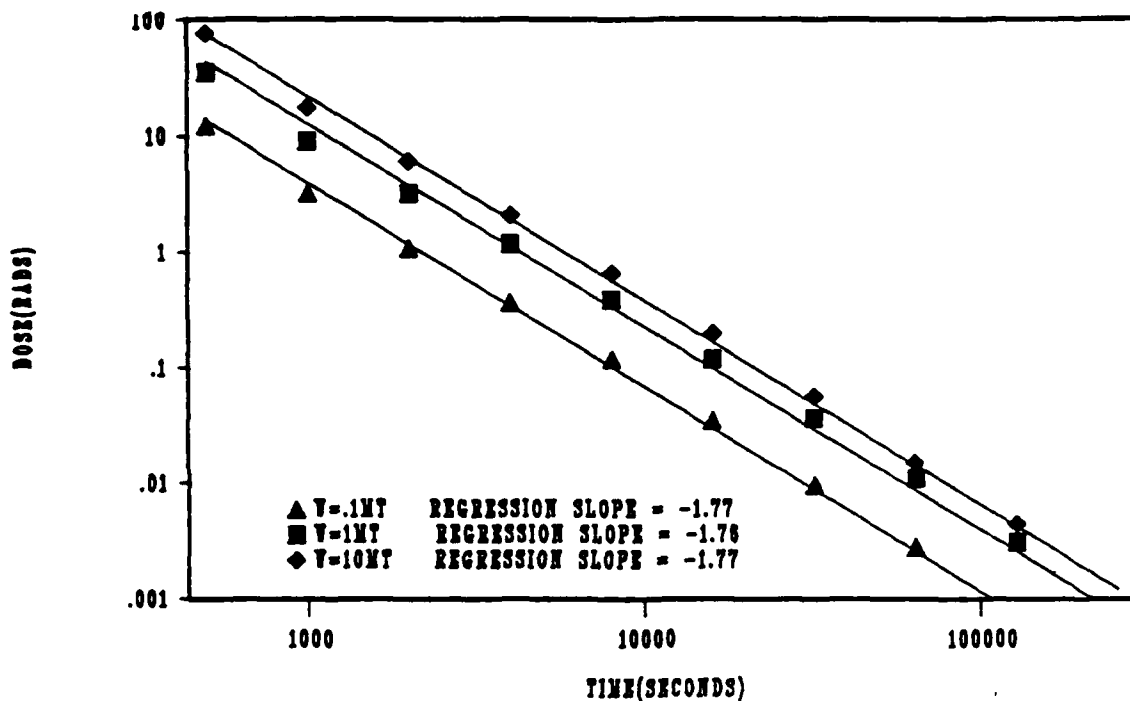


Figure 6. Dose vs. time near cloud top.
Flythrough (-40 km, 0, Ht, t-250)-(-40 km, 0, Ht, t+250)

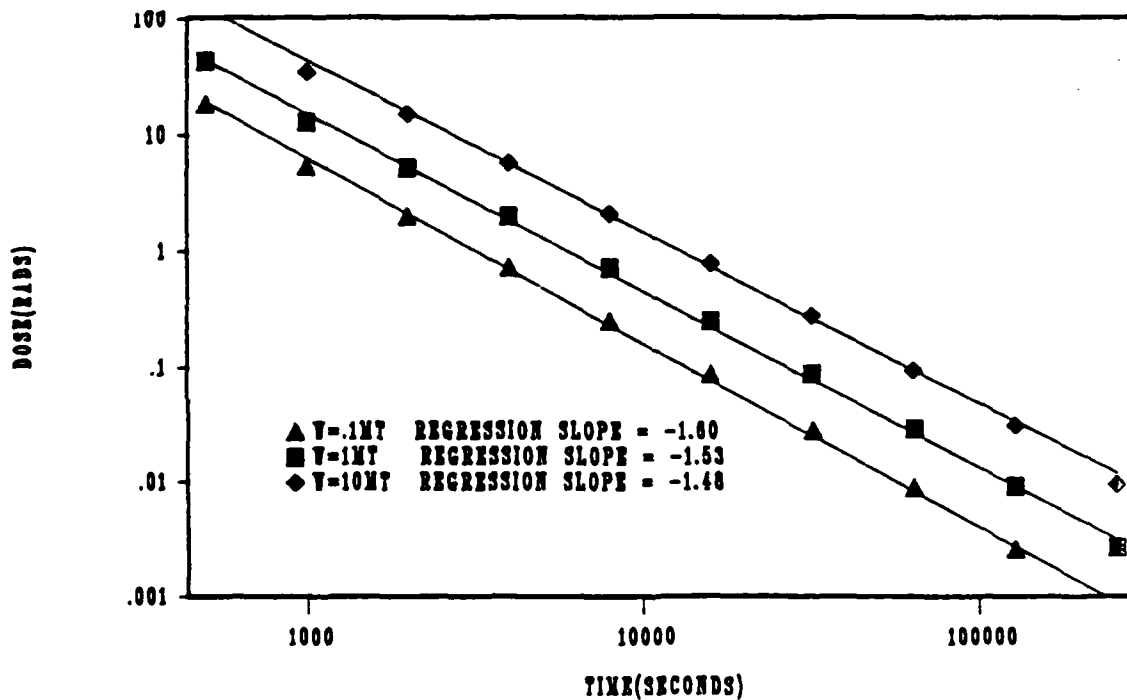


Figure 7. Dose vs. time near cloud base.
Flythrough (-40 km, 0, Hb, t-250)-(-40 km, 0, Hb, t+250).

particles are carried with the aircraft, the radiation from this source can become significant for extended missions. The gamma-radiation rate decays as:

$$R(t) = R_1 t^{-1.2} \quad (2)$$

where $R(t)$ is the radiation dose rate in rads/hour at time t hours after detonation and R_1 is the dose rate constant, equal to the dose rate at one hour after detonation (5). The evaluation of R_1 is based on the actual values of the total onboard dose rates at the corresponding cloud exit times of the aircraft. The calculated dose rate constants for trajectories near the cloud base and near the cloud top are given in Figures 8 and 9. A multiple regression fit to the data shows that the dose rate constant can be approximated by

$$R_1 = 1.44 W^{.55} t^{-.33} \quad (3)$$

where W is yield (megatons) and t is time (hours) after detonation that the plane reaches ground zero.

The total onboard radiation dose can be obtained by integrating equation (2) over the total time of the mission:

$$D(t) = \int_a^t R_1 t^{-1.2} dt = 5R_1 (t_a^{-0.2} - t^{-0.2}) \quad (4)$$

where $D(t)$ is the dose in rads for the mission at time t hours after detonation and t_a is the time after detonation that the aircraft exits the debris cloud.

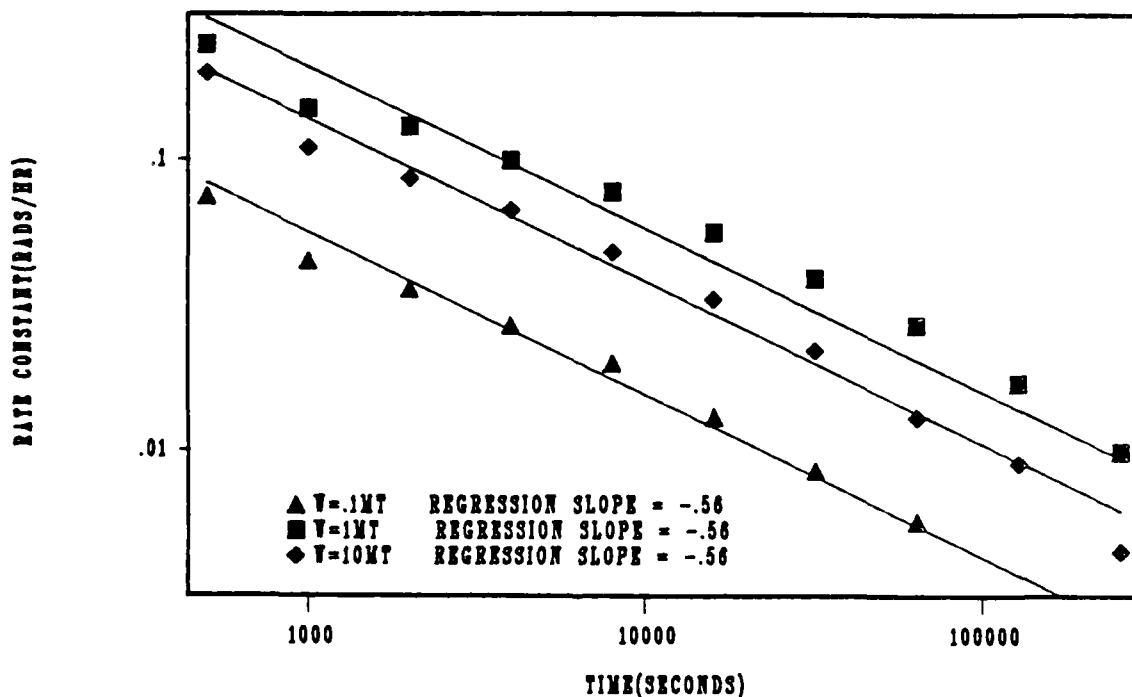


Figure 8. Rate constant vs. time near cloud top. Flythrough (-40 km, 0, Ht, t-250)-(40 km, 0, Ht, t+250).

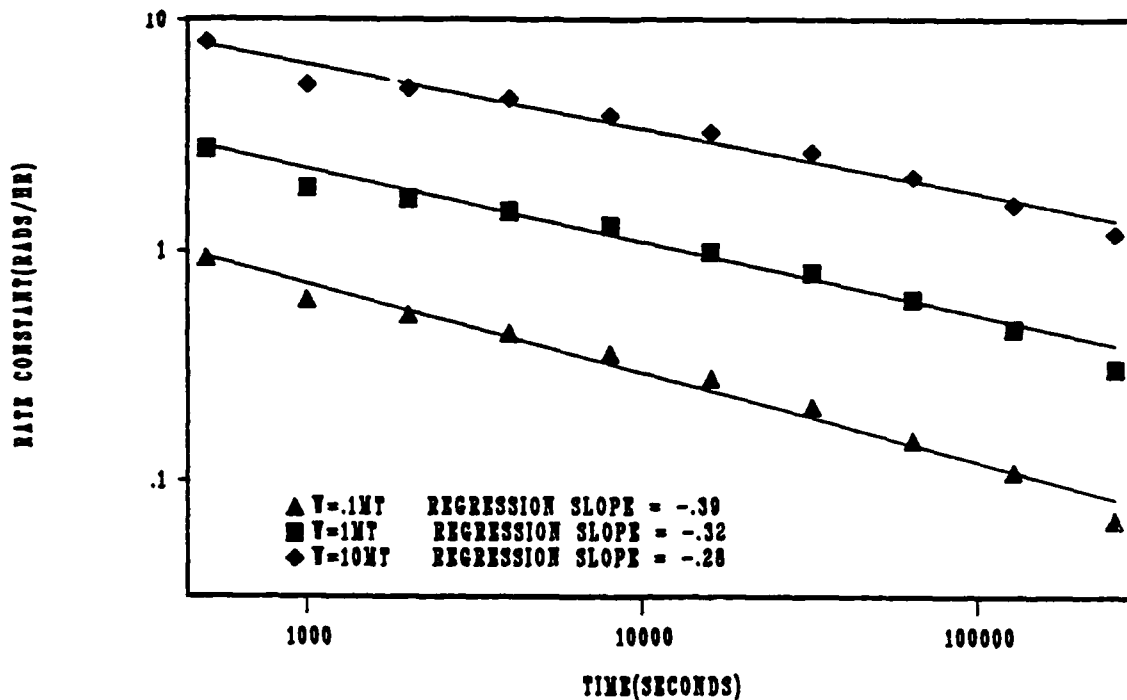


Figure 9. Rate constant vs. time near cloud base.
Flythrough (-40 km, Hb, t-250)-(40 km, 0, Hb, t+250).

CONCLUSIONS

The problem of radiation exposure to aircrews during or immediately after a nuclear attack is critical for USAF mission planners. The best way to reduce radiation exposure is for the aircraft to avoid the nuclear debris clouds. However, the size of the cloud or the number of clouds may preclude this option.

The CASSIE model will calculate the radiation doses to aircrews flying through the debris clouds from a few seconds after detonation to time of cloud disbursement. However, the residual nuclear radiation will not be the major concern for early times. The initial radiation, thermal effects, and the problems of flying through clouds of large debris particle sizes will be the major considerations. Thus, the results of this report should not be considered as feasible for flythrough times before cloud stabilization.

Radiation doses of aircrews flying through the nuclear debris clouds under various conditions have been calculated by the use of the CASSIE model for an aircraft moving with a constant speed of about 311 knots. The radiation dose for an aircraft moving at a different speed will change in an essentially inverse relationship with the speed of the aircraft. If an aircraft penetrates the cloud at a slower speed, the aircraft will be exposed to the radiation for a longer time and thus, the dose will increase. The adjusted dose, D_1 , is calculated by the equation:

$$D_1 = (311/v) D \quad (5)$$

where v is the actual speed of the aircraft in knots and D is the predicted dose that the aircraft would have had if it traveled at a speed of 311 knots. The error introduced by this approximation is less than 6% for a range of speeds of 200 to 700 knots at a flythrough time of 1 h. For later times or for speeds closer to 311 knots, this approximation is even better.

To illustrate the application of the results of this study, consider the following problem. An estimate of the radiation dose is desired for an aircraft flying through the middle of a debris cloud at the cloud base from a 0.5-MT surface burst with a flythrough speed of 250 knots at a time of 2000 s after detonation enroute to a target that requires 12 h for mission completion. The steps for this calculation are as follows:

(1) For the moment, consider the aircraft as having a speed of 311 knots. Calculate the radiation dose while immersed in the debris cloud from equation (1):

$$D = (2.34) (.5)^{0.48} (2000/3600)^{-1.53} \quad (6)$$

$$D = 4.1 \text{ rads}$$

(2) Find the onboard radiation dose rate constant from equation (3):

$$R_1 = (1.44) (.5)^{.55} (2000/3600)^{-0.33} \quad (7)$$

$$R_1 = 1.2 \text{ rads/hour}$$

(3) Find the onboard dose for a 12-h mission from equation (4):

$$D(12) = (5) (1.2) [(2000/3600)^{-2} - (12)^{-2}] \quad (8)$$

$$= 3.1 \text{ rads}$$

At this point multiply by the aircraft correction factor if known; see Appendix A.

(4) Calculate the total dose that the aircrew would experience by adding the results of steps (1) and (3):

$$\text{Total dose} = 7.2 \text{ rads}$$

(5) Adjust the dose to account for the speed of the aircraft by using equation (5):

$$D_1 = (311/250)(7.2) = 9.0 \text{ rads}$$

Thus, the predicted gamma-radiation dose to the aircrew is 9.0 rads for the mission. For 50 runs in the range .1 MT < W < 10 MT and 30 min < T < 1 day, the standard deviation of these predictions from the CASSIE predictions is 16%. Two runs deviated more than 30% from the CASSIE results.

If the aircraft flies through more than one cloud, the radiation dose of each cloud must be calculated separately. The total dose is the sum of all the individual doses.

ACKNOWLEDGMENTS

We gratefully acknowledge the encouragement and technical assistance of Colonel (Ret.) J. E. Pickering, chief of the Radiation Sciences Division of the USAF School of Aerospace Medicine, Brooks Air Force Base. Appreciation and thanks are also extended to Dr. R. A. Albanese, Mr. Earl Bell, ROTC Cadet William Berger, Dr. D. N. Farrer, and Dr. J. Taboada for their technical advice and support.

REFERENCES

1. Taboada, J., D. Hegedusich, and E. Bell. Interactive scenario computer model for dose rates to aircrew in flight through nuclear debris clouds. USAFSAM-TR-85-49, USAF School of Aerospace Medicine, Brooks AFB, Texas, July 1985.
2. Showers, R. L., and C. Crisco. User's manual for CASSANDRA: Cloud Snapshots of Dust Raised Aloft. Report ARBRL-TR-02116, Ballistic Research Laboratory, Aberdeen Proving Ground, MD, 1978.
3. Norment, H. G., DELFIC: Department of Defense fallout prediction system Vol I and II. Report DNA 5159F-1, Atmospheric Science Associates, MA, 1977.
4. Glasstone, S., and P. J. Dolan. The effects of nuclear weapons, 3d ed., p. 391. U.S. Government Printing Office, Washington D.C., 1977.
5. Way, K., and E. P. Wigner. The rate of decay of fission products. Phys Rev 73:1318 (1948).
6. Banks, J. E., Operation TEAPOT. Manned penetrations of atomic clouds, Project 2.8b. Report WT-1156 (EX), Air Force Special Weapons Center, Kirtland Air Force Base, NM, 1958.
7. Norment, H. G., Validation and Refinement of the DELFIC Cloud Rise Module. Report DNA 4320F, Atmospheric Science Associates, MA, 1977.

APPENDIX A

CORRECTION FOR AIRCRAFT PARAMETERS

To obtain the dose prediction outlined in the conclusions, the following aircraft parameters were arbitrarily chosen:

CL(cabin length) = 3205 cm (1300 in.)
CR(cabin radius) = 274 cm (110 in.)
DF(distance of crewmember to filter) = 250 cm (100 in.)
FR(air-flow rate into cabin) = 67.5 kg (150 lb)/min
PF(fraction of dust not trapped by filter) = .5

Given actual measurements of these 5 parameters, a correction factor for a particular type of aircraft may be calculated and the carryalong dose modified as follows:

1. Calculate the correction factor for cabin dimensions, C_{DM} :

$$C_{DM} = 147060[CL \cdot \text{LOG}(4CR^2 + CL^2) + 4CR \cdot \text{ATN}(CL/2CR) - 2CL \cdot \text{LOG}(CL)] / (CL \cdot CR^2)$$

2. Calculate the correction factor for crew distance from the filter, C_F :

$$C_F = 62500/D^2$$

3. Calculate the correction factor for air flow into the cabin, C_{FR} :

$$C_{FR} = FR/150$$

4. Calculate the correction factors for the fraction of dust allowed to pass into the cabin through the filter, C_{PF1} and C_{PF2} :

$$C_{PF1} = 2PF$$

$$C_{PF2} = 2(1-PF)$$

5. Calculate the combined correction factor, C :

$$C = 0.3 \cdot C_{PF1} C_{DM} C_{FR} + 0.7 \cdot C_{PF2} C_{FR} C_F$$

The carryalong dose (result of step 3 in the conclusions) is multiplied by this combined correction factor to obtain the corrected carryalong dose. The correction factor is based on: (a) analytical considerations discussed by Taboada et al.(1), and (b) the empirical observation that, given the arbitrary parameters originally chosen, the CASSIE model calculates that 30.% of the carryalong dose is due to dust trapped in the cabin while 70.% is due to dust trapped in the filter. The correction factor thus contributes no deviation of hand calculated results from CASSIE results.

APPENDIX B

EVALUATION OF MODEL ASSUMPTIONS

In the CASSIE model, the dose rate for a flythrough is calculated by the following steps.

- (1) Divide the flight path into a sequence of target points (x_1, y_1, z_1, t_1) , $(x_2, y_2, z_2, t_2), \dots, (x_n, y_n, z_n, t_n)$, each 4 km apart.
- (2) Calculate the dust concentration at each target point for each of 100 dust sizes using the CASSANDRA code.
- (3) Calculate the dose rate at each target point assuming:
 - (a) The rate contributed by a volume of space is proportional to the mass of dust contained therein.
 - (b) When the dose rate is calculated at a particular target point, the dust concentration is uniform and equal to the concentration at the target point.
 - (c) The cloud is considered to be infinite in extent for the purpose of integrating the dose rate for a target point.
- (4) Approximate the dose integration over the flight path by assuming:
 - (a) Constant velocity
 - (b) The dose rate varies linearly between target points.

Each of these operations contributes some error. An analysis of the extent of some of them follows.

Frequency of Target Points

A variety of flight paths were evaluated by taking points much closer together than 4 km (2.4 mi). The differences between these doses and the original dose were less than 5%. Thus, it was concluded that the 4 km (2.4 mi) interval for target points was a good compromise between accuracy and computer time.

Integration to get Gamma Rate

Taboada et al. (1) calculated the immersion dose rate D at a point (r_i) and time (t) by the following integral:

$$D(r_i) = t^{-1.2} K_1 \sum_{j=1}^{100} K(j) \int \frac{\rho(r, t, j) \exp(-K_2 |r - r_i|)}{4\pi |r - r_i|^2} dV \quad (B-1)$$

The space dependent portion of the gamma rate at any point for each dust size category is

$$D(r_i, j) = \text{Constant} \cdot \int \frac{\rho(r, j) \exp(-K_3 |r - r_i|)}{4\pi |r - r_i|^2} dV \quad (\text{B-2})$$

where r_i is the i th target point location, $\rho(r)$ is the dust density at location r , $K_3 = 6.767 \times 10^{-3}$ meters⁻¹ is the atmospheric absorption of a 1-MeV gamma photon, and j is the dust size category. The integral is taken over the volume of the cloud. If a coordinate transformation is made to put the origin at the target point and spherical coordinates are used, this equation becomes

$$D(r_i, j) = \text{Constant} \iiint \frac{\rho(s, j) \exp(-K_3 s)}{4\pi} \sin\theta \, d\theta \, d\phi \, ds \quad (\text{B-3})$$

If the assumptions in steps 3(b) and 3(c) are made, then $\rho(s) = \rho(r_i)$. Then, $\rho(s)$ is constant for purposes of evaluating the integral. Also, the cloud is spherically symmetric and infinite in size. Thus, the integral becomes

$$D(r_i, j) = \text{Constant} \rho(r_i, j) \int_0^{\infty} \exp(-K_3 s) \, ds \quad (\text{B-4})$$

$$D(r_i, j) = \text{Constant} \rho(r_i, j) / K_3 \quad (\text{B-5})$$

Two objections may occur at this point. First, the dust density does not continue indefinitely. This is not a serious problem because only 1% of the dose rate calculated by this approximation is due to any activity beyond a 680 m (2244 ft) sphere about r_i . That is,

$$\int_0^{680} \exp(-K_3 s) \, ds = .99 \int_0^{\infty} \exp(-K_3 s) \, ds \quad (\text{B-6})$$

A second objection is that $\rho(r)$ is not constant enough even within a 680 m (2244 ft) sphere to make a good approximation. To estimate the error incurred from the constant density approximation, an alternative integration scheme was performed, using the following symmetry argument. Consider the target point (x_i, y_i, z_i, t_i) . Poll the dust concentrations at 7 points: (x_i, y_i, z_i, t_i) , $(x_i \pm 200\text{m}, y_i, z_i, t_i)$, $(x_i, y_i \pm 200\text{m}, z_i, t_i)$ and $(x_i, y_i, z_i \pm 200\text{m}, t_i)$. Assume the dust concentration is uniform within a 100 m (327 ft) sphere around the target point. This region would encompass one-half the dose rate in the previous scheme. Divide the remaining space into 6 "congruent" (infinite) regions, each with axis of symmetry about the line through (x_i, y_i, z_i) and the respective polling point. This can be pictured by imagining the 8 points of a cube, $(x_i \pm d, y_i \pm d, z_i \pm d)$, on a hollow cantaloupe and slicing between them. Of course, this cantaloupe is infinite in radius. The intent of this division is to justify a weighting of the polled points. The dose rate due to one of the outside regions is one-twelfth of the rate calculated over all space if the dust concentration were uniformly equal to that of the polled point. In like manner, the interior sphere receives a one-half weighting.

The sequence of polling points $(x_1, y_1, z_1 + 200, t_1), \dots, (x_n, y_n, z_n + 200, t_n)$ creates a flight path 200 m (660 ft) above the original. The dose received from the upper outside region can be evaluated by running the original program and taking one-twelfth of the resulting dose. The same is true of $(x_1, y_1 \pm 200, z_1, t_1)$ and $(x_1, y_1, z_1 - 200, t_1)$. The other 2 outside integration regions $(x_1 \pm 200, y_1, z_1, t_1)$ form flight paths along the original path but shifted in time by 200 m (660 ft)/velocity, which is a negligible amount. It is assumed that the starting and ending points are outside the cloud.

Thus, the dose from this integration scheme is a linear function of 5 runs of the original program:

New dose estimate

$$\begin{aligned}
 = & (1/2 + 1/12 + 1/12) \text{ Dose } [(x_1, y_1, z_1, t_1) \rightarrow (x_n, y_n, z_n, t_n)] \\
 & + (1/12) \text{ Dose } [(x_1, y_1 + 200, z_1, t_1) \rightarrow (x_n, y_n + 200, z_n, t_n)] \\
 & + (1/12) \text{ Dose } [(x_1, y_1 - 200, z_1, t_1) \rightarrow (x_n, y_n - 200, z_n, t_n)] \quad (B-7) \\
 & + (1/12) \text{ Dose } [(x_1, y_1, z_1 + 200, t_1) \rightarrow (x_n, y_n, z_n + 200, t_n)] \\
 & + (1/12) \text{ Dose } [(x_1, y_1, z_1 - 200, t_1) \rightarrow (x_n, y_n, z_n - 200, t_n)]
 \end{aligned}$$

The doses predicted by CASSIE along the $(x_1, y_1 \pm 200, z_1, t_1) - (x_n, y_n \pm 200, z_n, t_n)$ flight paths do not differ from the prediction along the original path. As can be seen from Figure 3, doses along the $(x_1, y_1, z_1 \pm 200, t_1) - (x_n, y_n, z_n \pm 200, t_n)$ paths may differ by 25% from the prediction along the original path but both will not differ in the same direction from the original. The choice of one flight path, to differ by 25% while the other agrees with the original is a worst case and results in 25/12 or about 2% error. We take this as evidence that the original integration scheme is sufficiently accurate.

Calculation of Dust Densities

Results of CASSANDRA agree well with dust concentrations measured in the Dial Pack tests using conventional explosives. There are no measurements of airborne dust from detonations in the megaton range with which to compare the model's results. The cloud size discrepancy in the megaton range has already been noted. The lack of experimental data and other models for comparison makes the sources and amounts of error difficult to assess.

Atmospheric Conditions

The atmospheric winds are assumed to be zero. If nonzero winds are directed horizontally, the cloud will be translated as a unit if the winds are uniform and distorted if a wind shear exists. A wind shear along the direction of the flight path will cause little difference in dose while a perpendicular wind shear will produce a lower dose.

The effects of precipitation and large vertical air currents as in a thunderstorm are not considered. Precipitation will cause the dust particles to fall out earlier and thus, reduce doses from flythroughs.

Flight Through Cloud Center

The trajectories of the aircraft are assumed to pass over ground zero. If the aircraft passes a distance from ground zero, the radiation dose will be reduced by virtue of the aircraft spending less time inside the cloud and going through a lower dust concentration.